Sclera Force Control in Robot-assisted Eye Surgery: Adaptive Force Control vs. Auditory Feedback

Ali Ebrahimi,

Department of Mechanical Engineering and Laboratory for Computational Sensing and Robotics at the Johns Hopkins University, Baltimore, MD 21218 USA

Changyan He

Department of Mechanical Engineering and Laboratory for Computational Sensing and Robotics at the Johns Hopkins University, Baltimore, MD 21218 USA

School of Mechanical Engineering and Automation at Beihang University, Beijing, 100191 China.

Niravkumar Patel [Member, IEEE], **Marin Kobilarov**

Department of Mechanical Engineering and Laboratory for Computational Sensing and Robotics at the Johns Hopkins University, Baltimore, MD 21218 USA

Peter Gehlbach [Member, IEEE],

Wilmer Eye Institute, Johns Hopkins Hospital, Baltimore, MD 21287 USA

Iulian Iordachita [Senior Member, IEEE]

Department of Mechanical Engineering and Laboratory for Computational Sensing and Robotics at the Johns Hopkins University, Baltimore, MD 21218 USA

Abstract

Surgeon hand tremor limits human capability during microsurgical procedures such as those that treat the eye. In contrast, elimination of hand tremor through the introduction of microsurgical robots diminishes the surgeons tactile perception of useful and familiar tool-to-sclera forces. While the large mass and inertia of eye surgical robot prevents surgeon microtremor, loss of perception of small scleral forces may put the sclera at risk of injury. In this paper, we have applied and compared two different methods to assure the safety of sclera tissue during robot-assisted eye surgery. In the active control method, an adaptive force control strategy is implemented on the Steady-Hand Eye Robot in order to control the magnitude of scleral forces when they exceed safe boundaries. This autonomous force compensation is then compared to a passive force control method in which the surgeon performs manual adjustments in response to the provided audio feedback proportional to the magnitude of sclera force. A pilot study with three users indicate that the active control method is potentially more efficient.

aebrahi5@jhu.edu.

I. INTRODUCTION

Advancements in robot-assisted eye surgery have successfully reduced hand tremor and have potentially increased patient safety by enhancing tool tip precision during delicate eye surgery maneuvers. Two major categories of robots are presently used for this purpose, collaborative and telemanipulated. Collaborative robots share control of surgical tool with the surgeon. One such example is the Steady-Hand Eye Robot (SHER) developed at the Johns Hopkins University [1]. Using a co-manipulation control strategy and a design based on the Remote-Center-of-Motion (RCM), a 4-DoF (degrees of freedom) robot for retinal surgery was fabricated by Gijbels et al. [2], [3]. To obtain an adjustable pivot point, Nasseri et al. designed and developed a compact microsurgical system for ophthalmic surgery which can be mounted on patient's head [4], [5]. To increase dexterity in intraocular maneuvers, Wei et al. have also developed a hybrid two-armed robotic system [6].

Tele-manipulation robots have emerged as the most clinically ready configurations for retinal surgery at this time. Wilson et al. recently designed and built a novel master-slave intraocular robotic system capable of performing various surgical tasks [7]. Also, the University of Tokyo has developed a tele-operated system with which they executed different procedures including vitreous detachment and microcannulation. [8]–[10]. Furthermore, a microrobot for performing delicate procedures in retinal surgery was developed by Kummer et al. [11] which is controlled remotely with a wireless magnetic field.

The first in-human robot-assisted eye surgeries were performed by Edwards et al. [12] and Gijbels et al. [13] which can be considered as the most clinically advanced use of robots in eye surgery to date.

In manual eye surgery, surgeons usually rely on the visual and force feedback they attain when they are manipulating the eyeball. However, after introducing robots the interaction forces between the tool shaft and sclera (called sclera force Fig. 2) are no longer perceived by the surgeon. After doing a user study in robot-assisted eye manipulation, He et al. [14] reported an increase in the average scleral forces if not discerned by the surgeon may put the eyeball at high risk of injury. This would theoretically result from the large inertia and stiffness of the robot relative to the small and delicate tool-to-eye interaction forces. In order to enhance safety, the sensory information related to scleral forces has been restored in prior studies. Ebrahimi et al. [15] evaluated the advantage of providing haptic force feedback and audio feedback to surgeons based on sclera force. In another study, Cutler et al. assessed the effect of auditory feedback in restricting tool tip forces from going beyond safe levels in robot-assisted phantom membrane peeling task [16].

Based on previous studies, providing audio or haptic feedback to inform surgeons of unsafe levels of force have proven somewhat effective at keeping forces within safe ranges. However, the efficiency of audio or haptic feedback is highly dependent on the surgeon's response to them. As these methods are passive which means robot does not execute any autonomous action to correct unsafe forces. Furthermore, these passive methods of providing feedback may distract a surgeon's attention from the primary tasks of eye surgery

because the surgeon should continuously pay attention to them and be prepared to react properly. Therefore, implementing control methods in which the robot performs some or all of the safety actions autonomously may reduce the unsafe forces and prove beneficial in keeping the surgeon focused on primary surgical tasks.

In this paper, we have implemented an adaptive force control method by which the SHER autonomously decreases the magnitude of sclera force when it exceeds safe limits. In addition, we provided auditory feedback based on sclera force to implement a passive sclera force control. Finally, during a user study with three users, the efficiency of the active control of sclera force was compared to the passive audio force feedback.

This paper is organized as following. In section II, the way the active and the passive sclera force control have been implemented are explained. In section III, different components of experimental setup are explained. In section IV, the user study and the way the users are supposed to perform the experiments are delineated. Finally, the comparison results between the active and passive sclera force methods are discussed in section V.

II. Active and Passive Sclera Force Control

In this section we explain two different methods (active and passive) deployed to prevent the magnitude of sclera force from exceeding predetermined safe levels. The sclerotomy point (Fig. 1) is where the tool shaft leans on the eyeball. It is assumed there is no moment being applied form the sclera to the tool shaft at this point. In addition, the friction force between the sclerotomy and the tool shaft will produce a force component in the z direction of the end-effector (handle) frame (Fig. 2). This force is assumed to be negligible as well. Hence, only the terms F_{sx} and F_{sy} (depicted in Fig. 2) will contribute to the magnitude of sclera force, F_s (Fig. 2). Therefore, the equation for the magnitude of sclera force is written in (1):

$$F_s = \sqrt{F_{sx}^2 + F_{sy}^2} \tag{1}$$

In the active sclera force control strategy, the SHER is made to perform small movements autonomously to diminish F_s when it is going to overstep safe boundaries. This active control strategy is based on an adaptive force control method developed by Roy et. al [17] for a 1-DoF robot interacting with a compliant environment. We have built upon that control strategy and exploited it in order to make it applicable for 3-D sclera force control in robot-assisted eye surgery.

The second method is a passive control strategy in which we have utilized auditory feedback to warn the users about when F_s reaches unsafe levels. The efficiency of this sound-based sclera force control was already evaluated in [15] by our research group. After hearing the warning alarm, the surgeon needs to bring down the sclera force by reorienting the tool direction and executing corrective movements. These corrective movements should be performed simultaneously with the surgical tasks being done. This method is a passive control method because the robot does not perform any autonomous movements to counterbalance the sclera force exceeding safety boundaries. Thus, the surgeon alone adjusts sclera force in response to auditory feedback.

A. Adaptive force control

In order to control the sclera force with autonomous robot movement, an adaptive control strategy which was originally developed by [17], was extended to be applied to the SHER. Considering Fig. 3, the original adaptive control has the following purpose and assumptions:

Purpose:

- The purpose of the adaptive force control is to make the interaction force (F_e) applied to the robot (here the mass m shown in Fig. 3) by the environment with stiffness k to follow a desired pre-defined force F_d.

Assumptions:

- The 1-DoF robot has an inner loop velocity control which makes the robot velocity follow a desired velocity signal $\dot{X}_d$. In other words, the robot is a velocity-controlled robot.

- The robot is interacting with an environment with linear compliance $\lambda = \frac{1}{k}$ (based on Fig. 3, k is the environment stiffness) whose quantity is unknown to the force controller. In other words, the relation between the robot displacement $X - X_0$ and the force exerted by the compliant environment, F_e, is linear.

Roy et al. at [17] suggests that the control purpose mentioned above will be met under the following control law given in (2).

$$\dot{X}_d = \hat{\lambda}\dot{F}_d(t) - \alpha\Delta F(t) \tag{2}$$

In the equation above an estimation of the environment compliance λ is used because as mentioned the value of λ is unknown. This estimation is updated using the following adaptation law:

$$\dot{\hat{\lambda}} = -\Lambda\dot{F}_d(t)\Delta F(t) \tag{3}$$

In the equations (2) and (3) ΔF is the error of force control which is the difference between actual force F_e and the desired force F_d. The variables α and Λ are constant scalars, and $\dot{F}_d(t)$ is the derivative of the desired force signal. As shown in Fig. 4 which illustrates the block diagram for the 1-DoF adaptive force control, the signal $\dot{X}_d(t)$ which is produced in (2) is fed to the built-in velocity controller of the robot which is assumed to exist. At [17] it is proved using a Lyapunov function that the control input given in (2) and the adaptation law (3) will make the actual force between the robot and the environment, F_e, to converge to the desired force F_d. We have utilized this control algorithm in robot-assisted eye surgery to control the magnitude of sclera force, F_s, when it exceeds safety levels. The idea is to use the adaptive force control above to control each component of sclera force separately. Then, we would be able to make the robot autonomously reduce the magnitude of each component of sclera force (F_{sx} and F_{sy}) on desired paths resulting in decreasing F_s.

The SHER is a velocity-controlled robot interacting with a compliant environment that fulfills the above assumptions. The environment compliance is unknown to us which justifies the utilization of the adaptive force control. The robot is a 5-DoF manipulator three of which are translational ones which are just motions of the robot base along the Cartesian axis fixed in space. The other two rotational degrees of freedoms are the pitch and roll rotations of the end-effector mechanism which is shown at Fig. 5. The end-effector coordinate frame (handle frame) is attached to a fixed point on the tool shaft and is rigid to the end-effector mechanism which is shown in Fig. 5–b.

The normal impedance control of the robot makes it move in accordance with the forces and torques applied by the surgeon to the tool handle (the point where the surgeon grabs the tool, Fig. 5–b. This vector of forces and torques is denoted by $F_h^b \in \mathbb{R}^6$ which the superscript b indicates that the vector is projected in the handle frame explained above. Thus, for the normal impedance control of the robot, the desired translational and rotational velocities $\left(\dot{X}_d^b\right)$ of the end-effector frame is produced based on (4). The SHER is a velocity-conterolled robot and the embedded velocity controller of the robot is able to make the robot end-effector frame follow any bounded desired velocity vector $\dot{X}_d^b$

$$\dot{X}_d^b = \mathbb{K} F_h^b \tag{4}$$

In (4), the matrix $\mathbb{K} \in \mathbb{R}^{6 \times 6}$ is a constant diagonal gain matrix. The first three elements of $\dot{X}_d^b$ are the linear velocity of handle frame origin and the last three elements of $\dot{X}_d^b$ are the angular velocities of the handle frame. Hence, each of the six elements of $\dot{X}_d^b$ is related to its corresponding value in the force vector F_h^b Which means the robot obeys the way the surgeon wishes to manipulate the SHER.

In order to augment the sclera safety during eye manipulation, the adaptive controller (2) is integrated into (4) to generate the first two components of $\dot{X}_d^b$ which pertain to the x and y linear velocities of the handle frame origin. Then we can define decreasing desired reference signals for F_{sx} and F_{sy} to be followed. In other words, whenever F_s exceeds safe levels, the magnitude of both components of sclera force will be reduced based on the desired paths designed for the F_{sx} and F_{sy} using the adaptive force control method. Decreasing the magnitude of both components of sclera force will result in decreasing the sclera force magnitude F_s which has been the goal of active control of sclera force norm.

To encapsulate, equation set (5) are used whenever the autonomous norm control of sclera force is switched on (instead of using (4)). The scalar $\dot{X}_d^b[i]$ is the ith entry of the vector $\dot{X}_d^b$

$$
\begin{aligned}
\dot{X}_d^b[1] &= \hat{\lambda}_1 \dot{F}_{dx}(t) - \alpha_1 \Delta F_x(t) \\
\dot{X}_d^b[2] &= \hat{\lambda}_2 \dot{F}_{dy}(t) - \alpha_2 \Delta F_y(t) \\
\dot{X}_d^b[j] &= \mathbb{K}[jj] F_h^b[j] \quad \text{for } j = 3, 4, 5, 6
\end{aligned}
\tag{5}
$$

Where F_{dx} and F_{dy} are the desired reference signals for F_{sx} and F_{sy}, respectively. The terms ΔF_x and ΔF_y are also the tracking error for sclera force components which are $F_{sx} - F_{dx}$ and $F_{sy} - F_{dy}$, respectively. For the first two equations in (5), the adaptive laws to update the estimation for the environment compliance along the x and y directions of the body frame are given in (6).

$$\dot{\hat{\lambda}}_1 = -\Lambda_1 \dot{F}_{dx}(t) \Delta F_x(t)$$
$$\dot{\hat{\lambda}}_2 = -\Lambda_2 \dot{F}_{dy}(t) \Delta F_y(t)$$

(6)

Thus, when F_s goes beyond the upper safe level L, robot control equations are switched from (4) to (5) for autonomous reduction of sclera force. This, of course, does not stops the surgeon's manipulation because the last four elements of $\dot{X}_d^b$ are still produced based on the surgeon's interaction force F_h as it is apparent from (5).

The decreasing desired reference signals for F_{sx} and F_{sy} are written in (7).

$$F_{dx} = \frac{F_{sx}^0}{2}\left(e^{-a(t-t_0)} + 1\right)$$
$$F_{dy} = \frac{F_{sy}^0}{2}\left(e^{-a(t-t_0)} + 1\right)$$

(7)

where t_0 is the time when F_s reaches the upper safe bound of L and a is also a positive constant scalar representing how fast the desired trajectory falls. The scalars F_{sx}^0 and F_{sy}^0 are the values of F_{sx} and F_{sy} at time $t = t_0$. By little inspection, it is apparent that both of the desired trajectories defined above will make the magnitudes of F_{sx} and F_{sy} to decrease. Because, for example if F_{sx}^0 is positive, F_{dx} will be a decreasing signal and if F_{sx}^0 is negative F_{dx} will be an increasing signal. Thus, by these desired trajectories for F_{sx} and F_{sy}, F_s will also decrease and the safety of sclera force magnitude in robot-assisted eye manipulation will be guaranteed. If we keep the adaptive set of control equations (5), the magnitude of F_{sx} and F_{sy} will continuously decrease and the $t = \infty$ they will reach the constant values of $\frac{F_{sx}^0}{2}$ and $\frac{F_{sy}^0}{2}$, respectively. However, we want to switch back to the normal impedance control of the robot (4) as soon as possible since this control completely obeys the force F_h and feels more convenient to the surgeon. Thus, the control equations of (4) will again be applied when F_{sx} and F_{sy} reach $\frac{3F_{sx}^0}{4}$ and $\frac{3F_{sy}^0}{4}$ respectively which happens at a short finite time.

B. Auditory Substitution

For the purpose of passive sclera force control, auditory warning alarms in the form of beeps are provided to the surgeon when F_s reaches unsafe levels. As the surgeon hears the alarms, s/he should do corrective movements while s/he is performing surgical tasks to bring down the sclera force and get rid of the warning alarm. This method was used by our group in [15], and the advantage of providing audio feedback in enhancing safety was investigated.

Thus, for passive control of scelra force the surgeon does the eye manipulation while the impedance control equation set (4) is always implemented which means there is no switch to the equation set (5).

The first warning noise is sounded when $F_s > L_1$, and it is a low volume and low frequency noise. The second level of warning alarm is produced when $F_s > L_2$. When F_s reaches L_3 which is determined to be the unsafe level for F_s, a constant noise with relatively high volume is emitted to inform the surgeon of the safe bounds being passed. Thus, the first two emitted sounds produced at L_1 and L_2 act as a precaution for the unsafe level L_3 which is potentially harmful to sclera tissue.

III.   Experimental Setup and Method

To conduct experiments a setup which is depicted in Fig. 5 is prepared. The user should look though the microscope and hold the surgical tool which is also grasped by the robot to manipulate the eyeball. The eye phantom is placed in a 3-D printed eye socket. To measure the real-time value of F_{sx} and F_{sy}, a dual force-sensing tool which is built and calibrated based on [18] is used (see section III-B). Furthermore, the ATI force sensor (Fig. 5–b) is attached to the robot handle which measures the vector F_h^b To produce sound for the passive control method, two speakers are placed close to the user. Using the TCP/IP connection, data is transmitted between different modules of the system. Sclera force measurements, robot position, velocity and other required data are collected and manipulated through the software package (developed using the CISST framework, a collection of libraries for development of computer-assisted intervention systems; InfinityQS, Fairfax). The unsafe upper bound level of sclera force was set to be 120 mN according to what is explained in [15]. Therefore, we put the levels of L_1, L_2 and L_3 which were defined in the passive control of sclera force to be 80 mN, 100 mN and 120 mN, respectively. Thus, a soft alarm will be sounded at 80 mN, and it gradually merges into higher and rough warning noise when F_s reaches 120 mN.

For passive sclera control the warning alarms starts at 80 mN and progressively increases as we reach 120 mN. To have a fair comparison between the active and passive sclera control methods the same precaution idea is also applied for the active sclera control before reaching the unsafe upper bound of 120 mN. Thus, the adaptive control method is switched on when F_s reaches $L = 100$ mN. The control parameters are also specified as following. In (4) the diagonal matrix $\mathbb{K}$ is set to be $7.5\mathbb{I}$ where $\mathbb{I}$ is the identity matrix. In (5) and (6), the scalars a_1, a_2, Λ_1 are Λ_2 set to be 0.2, 0.2, 5×10^{-6} and 5×10^{-6}, respectively. To decide on the value of the parameter a in (7) we did some experiments to find an optimized value. We saw that for high values ($a \gg 1$) the robot was acting in a fast and unstable way. In contrast, for low values of a sclera forces were not following the desired trajectories well. Eventually, a was set to 1 to have a trade-off between stability and accuracy in force tracking error.

A.   Steady-Hand Eye Robot

The Steady-Hand Eye Robot is a cooperatively controlled 5-DoF robot for microsurgical manipulation in eye surgery that helps surgeons reduce hand tremor and have more stable, smooth and precise manipulations. As mentioned before, the SHER is a velocity-controlled

robot and the velocity of the motors of each joint is controlled by an embedded velocity controller (Galil 4088, Galil, 270 Technology Way, Rocklin, CA 95765).

B. Dual Force-Sensing Tool

To measure sclera forces F_{sx} and F_{sy}, FBG optical strain sensors were used as explained by [18]. The FBG sensors are very sensitive to strain which makes them suitable for applications measuring mN-order sclera forces. Three optical fibers were attached around a 25-gauge Nitinol wire at a separation angle of $120°$ from each other (see [18]). The FBG fibers are connected to an optical sensing interrogator (sm130–700 from Micron Optics Inc., Atlanta, GA) which sends the FBG raw optical data with a maximum frequency of 1 KH to the computer to calculate real-time force data (Fig. 5). In addition to measuring the components of sclera force, this tool design enables measuring tool tip force and the scalar value of insertion depth, as well. In this paper we utilize only the sclera force and we do not utilize the two other measured variables.

The calibration and validation processes for the tool measurement precision were carried out as previously reported by [18]. The mean square error for the sclera force and insertion depth measurements were calculated to be 3.8 mN and 0.29 mm, respectively.

C. Eye Phantom

The artificial silicon-made eye phantom is placed into a 3D-printed socket as shown in Fig. 1. To produce a realistic friction coefficient between the eye phantom and the socket, the surface between them is lubricated with mineral oil. In addition, phantom vessels which are just colored curves are printed on the posterior portion of the eyeball's interior.

IV. Pilot Study

In order to compare the efficacy of active and passive sclera force control methods in keeping the sclera force magnitude F_s below the unsafe level of 120 mN, we conducted a pilot study with three right-handed users. The research study attained the approval from the Johns Hopkins University Institutional Review Board for conducting user studies. The users were asked to hold the force-sensing tool attached to the robot with their right hand and move it collaboratively with the SHER to follow four colored vessels (Fig. 1) with the tool tip. A secondary but not-force-sensing tool is held in the left hand to facilitate the task (Fig. 1). However, we asked the users to use their right hand as the primary manipulation element. In [19], it is shown that in bimanual eye manipulation the dominant hand (here the right hand) applies significantly higher sclera forces.

Each user performed 10 trials for active sclera force control and 10 trials for passive sclera force control. In each trial, the permutation of the colored vessels to be followed is changed in a random way. During the manipulation the users were asked to view the eye through the microscope as a surgeon would in surgery. It is notable to say that user 1 was the most experienced while user 3 was the least experienced in operating the SHER.

V. Results and Discussion

In order to compare the two methods of sclera force control, some characteristic variables are defined. The first, is the total time required to complete the task of following four vessels. In order to quantify the augmentation of sclera force safety, the time spent with forces exceeding more than the upper safe boundary, 120 mN, is utilized. Also, the average value of sclera force and the maximum probable sclera force which is the force near where most of the time spent occurred during vessel following are calculated.

A typical trial for active control and audio feedback control of sclera force are depicted in Figs. 6 and 7, respectively. These figures just represents one of the trials done by user 3 which as mentioned before was the most novice user in working with the SHER.

As it is shown in Fig. 6, the robot is controlling the components of sclera force as the F_s exceeds 100 mN by decreasing the norm of F_{sx} and F_{sy}. It can be seen that F_s is mostly below the unsafe level, 120 mN, and in some cases it has a spike and goes in excess of the unsafe boundary, but the robot immediately brings it back to the safe region. However, if we look into the passive control method results in Fig. 7, it takes some time for the user to react to the warning alarm stating the unsafe level has been exceeded. Thus, more time is spent on forces more than 120 mN. Furthermore, another shortcoming of the audio feedback method is that, the user should always pay attention if an alarm is sounded and react to that promptly. This, may distract the user or in reality the surgeon's attention from the primary and absolutely delicate tasks of eye surgery. However, the active control method not only more enhances the safety of sclera force, but also does not disrupt the surgical tasks done by the surgeon and thus is always taking care of the sclera force norm during the surgery.

By looking into the results of Table I, it is observed that the time spent over 120 mN in active control method is significantly less than that for the audio norm control for all users. In other words, the active control method is acting more efficiently in preventing the sclera force from going beyond unsafe levels. User 1 who has the most experience in working with the SHER has zero time spent over 120 mN. For the most novice user which is user number 3, the ratio of the averaged time spent over 120 mN to the averaged total time of the experiment is as low as 4% for the active control method which means the sclera force in 96% of time is located in safe regions. Also, for all of the users, the average value of sclera force in the active control method is less than that quantity for the passive sclera force control.

Thus, active sclera force control enhances sclera force safety more than the other method without having the disadvantage of distracting the surgeon's attention. One drawback of the active sclera control is that the first two elements $\dot{X}_d^b$ are not obeying the user's interaction force F_h (according to (5)) which means the user does not have as much control over the robot's movements as compared to passive control method which has (4) as the governing control equations. However, the other last four elements of $\dot{X}_d^b$ are still abiding by F_h according to (5) which means the robot is mostly obeying the user commands rather than paying attention to the adaptive sclera force control. Thus, the user does not appreciate that the robot inhibits his/her commands. Nevertheless, user 3 stated that when the adaptive

control was switched on, the robot deviated a little from the direction he intended to move along. Thus, the control parameters require further optimization in order to impart minimal impedance to the surgeon while protecting the eye from scleral force injury. Finally, we did not observe any instability during the experiments due to switching between control methods, but one of our future goals is to further investigate the stability of the switching system.

Acknowledgments

References

[1]. Üneri A, Balicki MA, Handa J, Gehlbach P, Taylor RH, and Iordachita I, "New steady-hand eye robot with micro-force sensing for vitreoretinal surgery," in Biomedical Robotics and Biomechatronics (BioRob), 2010 3rd IEEE RAS and EMBS International Conference on. IEEE, 2010, pp. 814–819.

[2]. Gijbels A, Wouters N, Stalmans P, Van Brussel H, Reynaerts D, and Vander Poorten E, "Design and realisation of a novel robotic manipulator for retinal surgery," in Intelligent Robots and Systems (IROS), 2013 IEEE/RSJ International Conference on. IEEE, 2013, pp. 3598–3603.

[3]. Willekens K, Gijbels A, Schoevaerdts L, Esteveny L, Janssens T, Jonckx B, Feyen JH, Meers C, Reynaerts D, Vander Poorten E et al., "Robot-assisted retinal vein cannulation in an in vivo porcine retinal vein occlusion model," Acta ophthalmologica, vol. 95, no. 3, pp. 270–275, 2017. [PubMed: 28084059]

[4]. Nasseri MA, Eder M, Nair S, Dean E, Maier M, Zapp D, Lohmann CP, and Knoll A, "The introduction of a new robot for assistance in ophthalmic surgery," in 2013 35th Annual International Conference of the IEEE Engineering in Medicine and Biology Society (EMBC). IEEE, 2013, pp. 5682–5685.

[5]. Nasseri MA, Eder M, Eberts D, Nair S, Maier M, Zapp D, Lohmann CP, and Knoll A, "Kinematics and dynamics analysis of a hybrid parallel-serial micromanipulator designed for biomedical applications," in 2013 IEEE/ASME International Conference on Advanced Intelligent Mechatronics. IEEE, 2013, pp. 293–299.

[6]. Wei W, Goldman R, Simaan N, Fine H, and Chang S, "Design and theoretical evaluation of micro-surgical manipulators for orbital manipulation and intraocular dexterity," in Robotics and Automation, 2007 IEEE International Conference on. IEEE, 2007, pp. 3389–3395.

[7]. Wilson JT, Gerber MJ, Prince SW, Chen C-W, Schwartz SD, Hubschman J-P, and Tsao T-C, "Intraocular robotic interventional surgical system (iriss): Mechanical design, evaluation, and master–slave manipulation," The International Journal of Medical Robotics and Computer Assisted Surgery, vol. 14, no. 1, p. e1842, 2018.

[8]. Ueta T, Yamaguchi Y, Shirakawa Y, Nakano T, Ideta R, Noda Y, Morita A, Mochizuki R, Sugita N, Mitsuishi M et al., "Robot-assisted vitreoretinal surgery: Development of a prototype and feasibility studies in an animal model," Ophthalmology, vol. 116, no. 8, pp. 1538–1543, 2009. [PubMed: 19545902]

[9]. Noda Y, Ida Y, Tanaka S, Toyama T, Roggia MF, Tamaki Y, Sugita N, Mitsuishi M, and Ueta T, "Impact of robotic assistance on precision of vitreoretinal surgical procedures," PloS one, vol. 8, no. 1, p. e54116, 2013. [PubMed: 23335991]

[10]. Tanaka S, Harada K, Ida Y, Tomita K, Kato I, Arai F, Ueta T, Noda Y, Sugita N, and Mitsuishi M, "Quantitative assessment of manual and robotic microcannulation for eye surgery using new eye model," The International Journal of Medical Robotics and Computer Assisted Surgery, vol. 11, no. 2, pp. 210–217, 2015. [PubMed: 24737776]

[11]. Kummer MP, Abbott JJ, Kratochvil BE, Borer R, Sengul A, and Nelson BJ, "Octomag: An electromagnetic system for 5-dof wireless micromanipulation," IEEE Transactions on Robotics, vol. 26, no. 6, pp. 1006–1017, 2010.

[12]. Edwards T, Xue K, Meenink H, Beelen M, Naus G, Simunovic M, Latasiewicz M, Farmery A, de Smet M, and MacLaren R, "First-in-human study of the safety and viability of intraocular robotic surgery," Nature Biomedical Engineering, p. 1, 2018.

[13]. Gijbels A, Smits J, Schoevaerdts L, Willekens K, Vander Poorten EB, Stalmans P, and Reynaerts D, "In-human robot-assisted retinal vein cannulation, a world first," Annals of Biomedical Engineering, pp. 1–10, 2018.

[14]. He C, Ebrahimi A, Roizenblatt M, Patel N, Yang Y, Gehlbach PL, and Iordachita I, "User behavior evaluation in robot-assisted retinal surgery," in 2018 27th IEEE International Symposium on Robot and Human Interactive Communication (RO-MAN). IEEE, 2018, pp. 174–179.

[15]. Ebrahimi A, He C, Roizenblatt M, Patel N, Sefati S, Gehlbach P, and Iordachita I, "Real-time sclera force feedback for enabling safe robot-assisted vitreoretinal surgery," in 2018 40th Annual International Conference of the IEEE Engineering in Medicine and Biology Society (EMBC), 7 2018, pp. 3650–3655.

[16]. Cutler N, Balicki M, Finkelstein M, Wang J, Gehlbach P, Mc-Gready J, Iordachita I, Taylor R, and Handa JT, "Auditory force feedback substitution improves surgical precision during simulated ophthalmic surgery," Investigative ophthalmology & visual science, vol. 54, no. 2, pp. 1316–1324, 2013. [PubMed: 23329663]

[17]. Roy J and Whitcomb LL, "Adaptive force control of position/velocity controlled robots: theory and experiment," IEEE Transactions on Robotics and Automation, vol. 18, no. 2, pp. 121–137, 2002.

[18]. He X, Balicki M, Gehlbach P, Handa J, Taylor R, and Iordachita I, "A multi-function force sensing instrument for variable admittance robot control in retinal microsurgery," in Robotics and Automation (ICRA), 2014 IEEE International Conference on. IEEE, 2014, pp. 1411–1418.

[19]. He C, Roizenblatt M, Patel N, Ebrahimi A, Yang Y, Gehlbach P, and Iordachita I, "Towards bimanual robot-assisted retinal surgery:tool-to-sclera force evaluation," in SENSORS, 2018 IEEE. IEEE, 2018, pp. 1701–1704.
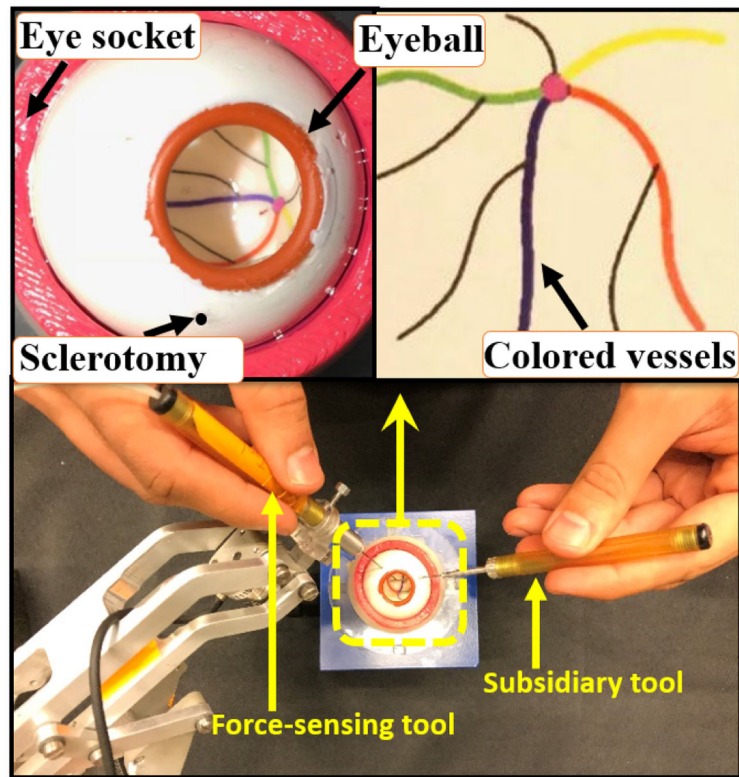
Fig. 1.
(Bottom) an illustration of how users hold the tools to manipulate the eye. (Top) close-up views of the eyeball and the phantom colored vessels.
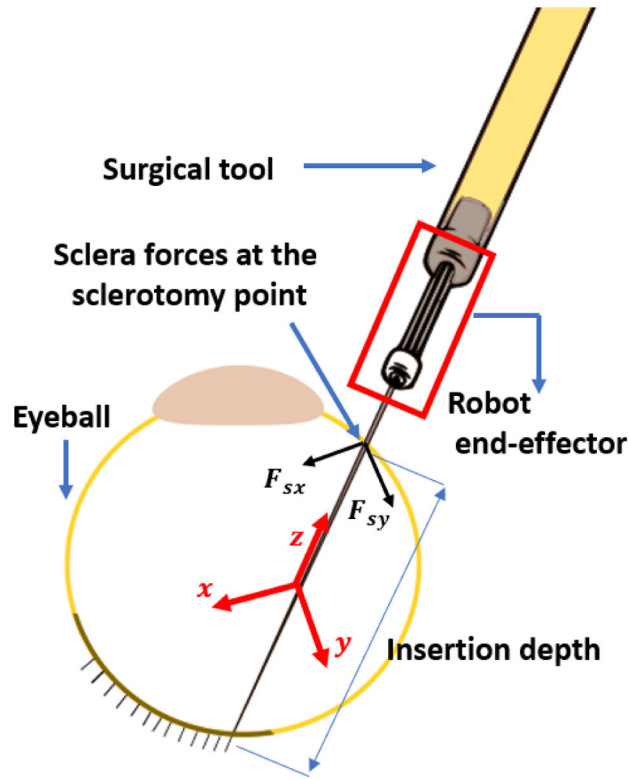
Fig. 2.
Schematic diagram for tool and eyball interaction. Sclera force components (F_{sx} and F_{sy}) are perpendicular to the tool shaft and expressed in the end-effector coordinate frame (the red coordinate frame whose origin is at a fixed point on the tool shaft and is rigid to the end-effector and the tool). Tool insertion depth is the length of the tool inserted inside the eye.
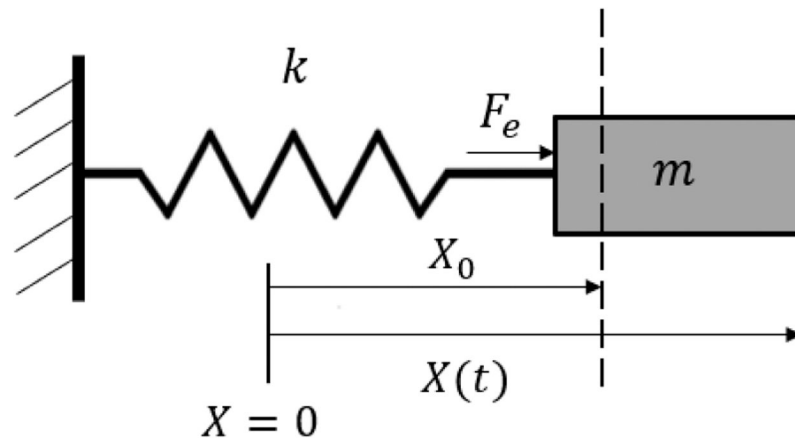
Fig. 3.
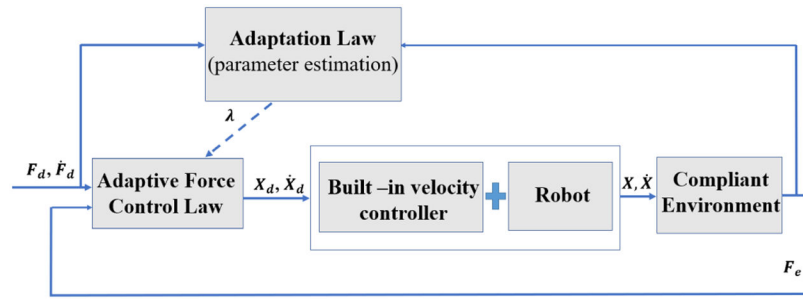A 1-DoF robot with mass *m* interacting with an environment with stiffness *k*

Fig. 4.
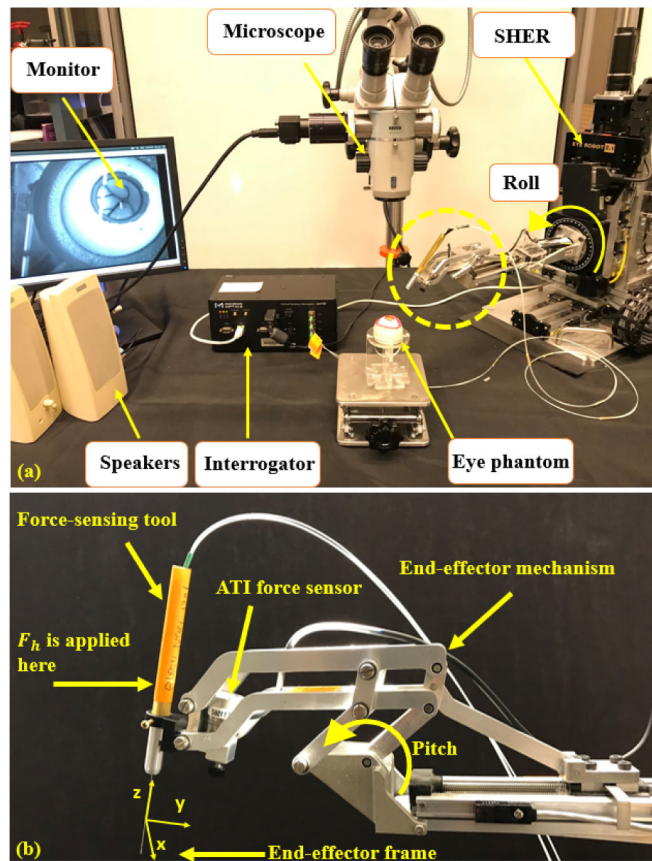Block diagram for the 1-DoF adaptive force controller

Fig. 5.
(a) Experimental setup showing: SHER, FBG interrogator for the force sensing tool, microscope for looking into the eye phantom and speakers to provide the audio feedback. (b) The close-up view for the dashed circle in (a).
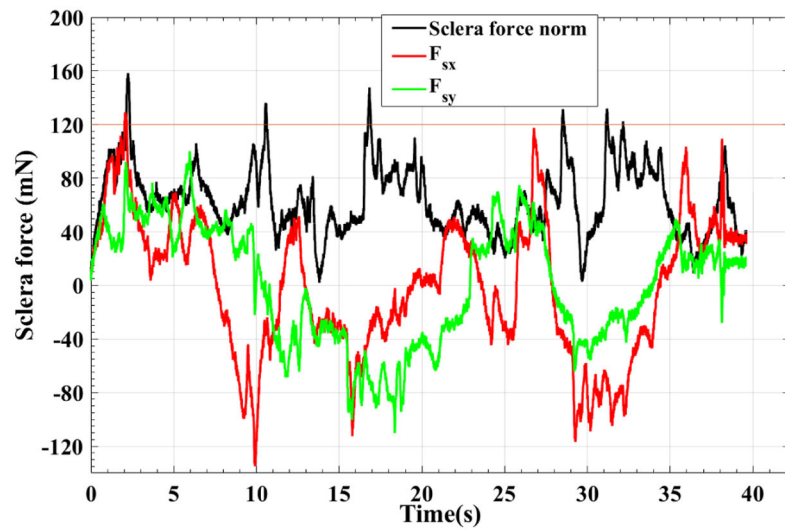
Fig. 6.
A characteristic plot for F_{sx}, F_{sy} and F_s of one of the 10 trials done by user 3. For this trial the adaptive norm control of sclera force was implemented.
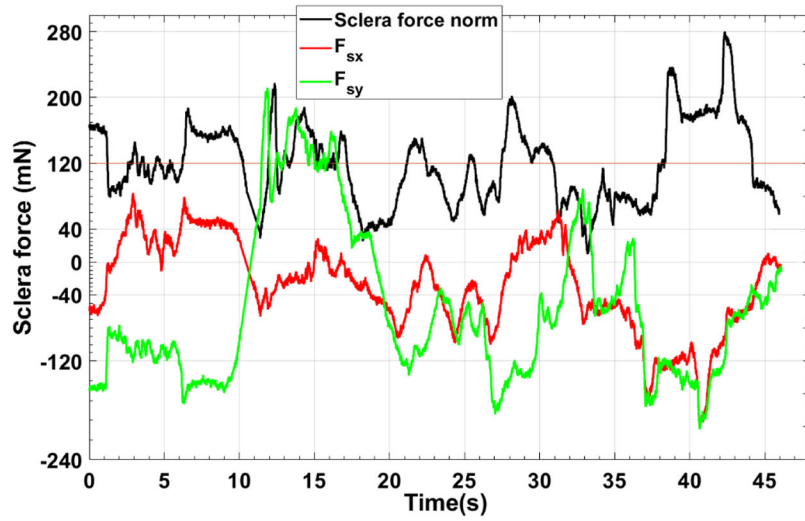
Fig. 7.
A characteristic plot for F_{sx}, F_{sy} and F_s of one of the 10 trials done by user 3. For this trial the passive control of sclera force was implemented.

TABLE I:

Average results for each of the three users in the pilot study. For each user the results are averaged over the 10 trials done by the user for that specific task. The numbers in parenthesis are standard deviation

Control Paradigm	Mean of sclera force (mN)	Max probable sclera force (mN)	Average total time (s)	Time spent over 120 mN(s)	Percent of time spent over 120 mN
User 1					
Active control	61.8(24.9)	84	40.5 (6.8)	0	0
Passive control	74.6 (42.3)	53	40.2 (5.2)	5.2 (1.6)	13%
User 2					
Active control	66.5 (25.98)	64	26.0 (1.8)	0.47 (0.32)	2%
Passive control	70.32 (38.6)	44	28.3 (4.4)	3.4 (1.8)	12%
User 3					
Active control	67.98 (29.0)	65	47.7 (9.94)	2.1 (0.75)	4%
Passive control	102.12 (57.8)	84	45.4 (11.2)	15.7 (8.3)	35%